

June 13, 2018

# Hole Photoproduction in Insulating Copper Oxide

O. P. Sushkov<sup>a,b</sup>, G. Sawatzky, R. Eder, and H. Eskes

*Materials Science Center, University of Groningen*

*Nijenborgh 4, 9747 AG Groningen*

*The Netherlands*

## Abstract

To explain the experimental spectra for angle resolved photoemission we consider a modified  $t - J$  model. The modified model includes next nearest ( $t'$ ) and next next nearest ( $t''$ ) hopping as well as Hubbard model corrections to the spectral weights. A Dyson equation which relates the single hole Green's functions for a given pseudospin and given spin is derived and is compared to experimental results.

PACS numbers: 75.50.Ee, 75.10.Jm,

## I. INTRODUCTION

Recent angle resolved photoemission (ARPES) measurements by Wells *et al*<sup>1</sup> and by Pothuizen *et al*<sup>2</sup> for insulating Copper Oxide  $\text{Sr}_2\text{CuO}_2\text{Cl}_2$  provide a unique possibility to experimentally determine the single hole properties. In the frameworks of a  $t - t' - J$  model the problem has been analyzed by Nazarenko *et al*<sup>3</sup> using a cluster method and Bala, Oles, and Zaanen<sup>4</sup> using a self-consistent Born approximation (SCBA). It was demonstrated in these works that including  $t'$  hopping improves agreement with experiment, but a complete description of the ARPES spectra especially the  $k$  dependent intensity was not achieved.

In the present work we consider a  $t - t' - t'' - J$  model. A Dyson equation which relates the one electron Green's function measured in experiment to the hole Green's function found in the self-consistent Born approximation is derived. We also introduce into this equation the corrections which originate from finite  $U$  as in the Hubbard model. With parameters taken from LDA band calculations by Andersen *et al*<sup>5</sup> we got a reasonably good description of the experimental ARPES spectra. The results are sensitive to  $t''$ . The parameter  $t'$  is less important. The importance of  $t''$  was also pointed out by Belinicher and Chernyshev<sup>6</sup>. For the explanation of width of ARPES spectra we need to introduce additional broadening and possible origins of this are discussed.

The Hamiltonian of  $t - t' - t'' - J$  model is of the form

$$H = -t \sum_{\langle ij \rangle \sigma} c_{i\sigma}^\dagger c_{j\sigma} - t' \sum_{\langle ij_1 \rangle \sigma} c_{i\sigma}^\dagger c_{j_1\sigma} - t'' \sum_{\langle ij_2 \rangle \sigma} c_{i\sigma}^\dagger c_{j_2\sigma} + J \sum_{\langle ij \rangle} \mathbf{S}_i \mathbf{S}_j. \quad (1)$$

$c_{i\sigma}^\dagger$  is the creation operator of an electron with spin  $\sigma$  ( $\sigma = \uparrow, \downarrow$ ) at site  $i$  of the two-dimensional square lattice, the  $\langle ij \rangle$  represents nearest neighbor sites,  $\langle ij_1 \rangle$  - next nearest neighbor (diagonal), and  $\langle ij_2 \rangle$  represents next next nearest sites. The spin operator is  $\mathbf{S}_i = \frac{1}{2} c_{i\alpha}^\dagger \sigma_{\alpha\beta} c_{i\beta}$ . The size of the exchange measured in two magnon Raman scattering<sup>7,8</sup> is  $J = 125\text{meV}$ . The most recent calculation of the hopping matrix elements has been done by Andersen *et al*<sup>5</sup>. They consider a two-plane situation and the effective matrix elements are slightly different for symmetric and antisymmetric combinations of orbitals between planes. After averaging over these combinations we get:  $t = 386\text{meV}$ ,  $t' = -105\text{meV}$ ,  $t'' = 86\text{meV}$ . Below we set  $J = 1$ , in these units

$$t = 3.1, \quad t' = -0.8, \quad t'' = 0.7 \quad (2)$$

## II. HOLE GREEN'S FUNCTION WITH FIXED PSEUDOSPIN. SELF-CONSISTENT BORN APPROXIMATION (SCBA)

It is well known that at half filling (one electron per site) the model under consideration is equivalent to a Heisenberg model. It represents a Mott insulator with long range antiferromagnetic order. We denote the corresponding ground state wave function by  $|0\rangle$ . We are interested in the situation when one electron is removed from this state, so a single hole is produced. The dynamics of a single hole in the antiferromagnetic background can be described by SCBA<sup>9,10</sup>. This approximation works very well due to the absence of a single loop correction to the hole-spin-wave vertex<sup>11–13</sup>. Let us recall the idea of this approximation. The bare hole operator  $d_i$  is defined so that  $d_i^\dagger \propto c_{i\uparrow}$  on the  $\uparrow$  sublattice and  $\propto c_{i\downarrow}$  on the  $\downarrow$  sublattice. In the momentum representation

$$d_{\mathbf{k}\downarrow}^\dagger = \sqrt{\frac{2}{N(1/2+m)}} \sum_{i\in\uparrow} c_{i\uparrow} e^{i\mathbf{k}\mathbf{r}_i}, \quad d_{\mathbf{k}\uparrow}^\dagger = \sqrt{\frac{2}{N(1/2+m)}} \sum_{j\in\downarrow} c_{j\downarrow} e^{i\mathbf{k}\mathbf{r}_j}. \quad (3)$$

$N$  is number of sites,  $m = |\langle 0 | S_{iz} | 0 \rangle| \approx 0.3$  is the average sublattice magnetization. The quasi-momentum  $\mathbf{k}$  is limited to be inside the magnetic Brillouin zone:  $\gamma_{\mathbf{k}} = \frac{1}{2}(\cos k_x + \cos k_y) \geq 0$ . In this notations it looks like  $d_{\mathbf{k}\sigma}$  has spin  $\sigma = \pm 1/2$ , but actually rotation invariance is violated and  $\sigma$  is a pseudospin which denotes the sublattice. Nevertheless the pseudospin gives the correct value of the spin  $z$ -projection:  $S_z = \sigma = \pm 1/2$ . The coefficients in (3) provide the correct normalization:

$$\langle 0 | d_{\mathbf{k}\downarrow} d_{\mathbf{k}\downarrow}^\dagger | 0 \rangle = \frac{2}{N(1/2+m)} \sum_{i\in\uparrow} \langle 0 | c_{i\uparrow}^\dagger c_{i\uparrow} | 0 \rangle = \frac{1}{1/2+m} \langle 0 | \frac{1}{2} + S_{iz} | 0 \rangle = 1. \quad (4)$$

The hole Green's function is defined as

$$G_d(\epsilon, \mathbf{k}) = -i \int \langle 0 | T d_{\mathbf{k}\sigma}(\tau) d_{\mathbf{k}\sigma}^\dagger(0) | 0 \rangle e^{i\epsilon\tau} d\tau \quad (5)$$

The  $t'$ ,  $t''$  terms in the Hamiltonian (1) correspond to the hole hopping inside one sublattice. This gives the bare hole dispersion

$$\epsilon_{0\mathbf{k}} = 4t' \cos k_x \cos k_y + 2t'' (\cos 2k_x + \cos 2k_y) \rightarrow \beta_{01} \gamma_{\mathbf{k}}^2 + \beta_{02} (\gamma_{\mathbf{k}}^-)^2, \quad (6)$$

where  $\gamma_{\mathbf{k}}^- = \frac{1}{2}(\cos k_x - \cos k_y)$ ,  $\beta_{01} = 4(2t'' + t')$ , and  $\beta_{02} = 4(2t'' - t')$ . In equation (6) we took into account that the sign of a hole dispersion is opposite to that for an electron (maximum of electron band correspond to minimum of hole band), and omitted some constant. The bare hole Green's function is

$$G_{0d}(\epsilon, \mathbf{k}) = \frac{1}{\epsilon - \epsilon_{0\mathbf{k}} + i0}. \quad (7)$$

For spin excitations the usual linear spin-wave theory is used (see, e.g. review paper<sup>14</sup>). It is convenient to have two types of spin-waves,  $\alpha_{\mathbf{q}}^\dagger$  with  $S_z = -1$ , and  $\beta_{\mathbf{q}}^\dagger$  with  $S_z = +1$ , and  $\mathbf{q}$  restricted to be inside the magnetic Brillouin zone.

$$\begin{aligned} \sqrt{\frac{2}{N}} \sum_{i \in \uparrow} S_i^+ e^{-i\mathbf{qr}_i} &\approx u_{\mathbf{q}} \alpha_{\mathbf{q}} + v_{\mathbf{q}} \beta_{-\mathbf{q}}^\dagger, \\ \sqrt{\frac{2}{N}} \sum_{j \in \downarrow} S_j^- e^{i\mathbf{qr}_j} &\approx v_{\mathbf{q}} \alpha_{\mathbf{q}}^\dagger + u_{\mathbf{q}} \beta_{-\mathbf{q}}. \end{aligned} \quad (8)$$

The spin-wave dispersion and parameters of Bogoliubov transformation diagonalizing the spin-wave Hamiltonian are:

$$\begin{aligned} \omega_{\mathbf{q}} &= 2\sqrt{1 - \gamma_{\mathbf{q}}^2}, \\ u_{\mathbf{q}} &= \sqrt{\frac{1}{\omega_{\mathbf{q}}} + \frac{1}{2}}, \\ v_{\mathbf{q}} &= -\text{sign}(\gamma_{\mathbf{q}}) \sqrt{\frac{1}{\omega_{\mathbf{q}}} - \frac{1}{2}}. \end{aligned} \quad (9)$$

Hopping to nearest a neighbor in the Hamiltonian (1) gives an interaction of the hole with spin-waves.

$$H_{h,sw} = \sum_{\mathbf{k}, \mathbf{q}} g_{\mathbf{k}, \mathbf{q}} \left( d_{\mathbf{k}+\mathbf{q}\downarrow}^\dagger d_{\mathbf{k}\uparrow} \alpha_{\mathbf{q}} + d_{\mathbf{k}+\mathbf{q}\uparrow}^\dagger d_{\mathbf{k}\downarrow} \beta_{\mathbf{q}} + H.c. \right), \quad (10)$$

with vertex  $g_{\mathbf{k}, \mathbf{q}}$  given by

$$\begin{aligned} g_{\mathbf{k}, \mathbf{q}} &\equiv \langle 0 | \alpha_{\mathbf{q}} d_{\mathbf{k}\uparrow} | H_t | d_{\mathbf{k}+\mathbf{q}\downarrow}^\dagger | 0 \rangle = \\ &= \frac{2}{N(1/2 + m)} \langle 0 | \alpha_{\mathbf{q}} \sum_{\langle i \in \uparrow, j \in \downarrow \rangle} e^{-i\mathbf{kr}_j} c_{j\downarrow}^\dagger \left( -t c_{i\sigma}^\dagger c_{j\sigma} \right) c_{i\uparrow} e^{i(\mathbf{k}+\mathbf{q})\mathbf{r}_i} | 0 \rangle = \\ &= \frac{2}{N(1/2 + m)} t \sum_{\langle i \in \uparrow, j \in \downarrow \rangle} e^{-i\mathbf{kr}_j + i(\mathbf{k}+\mathbf{q})\mathbf{r}_i} \left( \langle 0 | \alpha_{\mathbf{q}} c_{j\downarrow}^\dagger c_{j\uparrow} c_{i\uparrow}^\dagger c_{i\uparrow} | 0 \rangle + \langle 0 | \alpha_{\mathbf{q}} c_{j\downarrow}^\dagger c_{j\downarrow} c_{i\downarrow}^\dagger c_{i\uparrow} | 0 \rangle \right) \approx \\ &\approx \frac{2}{N} t \sum_{\langle i \in \uparrow, j \in \downarrow \rangle} e^{-i\mathbf{kr}_j + i(\mathbf{k}+\mathbf{q})\mathbf{r}_i} \langle 0 | \alpha_{\mathbf{q}} \left( S_j^- + S_i^- \right) | 0 \rangle = 4t \sqrt{\frac{2}{N}} (\gamma_{\mathbf{k}} u_{\mathbf{q}} + \gamma_{\mathbf{k}+\mathbf{q}} v_{\mathbf{q}}). \end{aligned} \quad (11)$$

In this calculation we have used the usual mean field ground state factorization approximation:  $\langle 0 | \alpha_{\mathbf{q}} c_{j\downarrow}^\dagger c_{j\uparrow} c_{i\uparrow}^\dagger c_{i\uparrow} | 0 \rangle \approx \langle 0 | \alpha_{\mathbf{q}} c_{j\downarrow}^\dagger c_{j\uparrow} | 0 \rangle \langle 0 | c_{i\uparrow}^\dagger c_{i\uparrow} | 0 \rangle = \langle 0 | \alpha_{\mathbf{q}} S_j^- | 0 \rangle (1/2 + m)$ . The vertex  $g_{\mathbf{k}, \mathbf{q}}$  is independent of  $t'$ ,  $t''$  because these parameters correspond to hopping inside one sublattice. The form of the vertex  $g_{\mathbf{k}, \mathbf{q}}$  is well known. The actual purpose of calculation (11)

is to demonstrate that  $g_{\mathbf{k},\mathbf{q}}$  is valid in a more general situation than it is usually believed. It is independent of the particular value of the sublattice magnetization  $m$ . Therefore, for example,  $g_{\mathbf{k},\mathbf{q}}$  remains the same in the presence of strong additional frustrations.

One can easily prove that the spin structure of the interaction (10) forbids single loop corrections to the hole-spin-wave vertex and, as usually, the two loop correction is small numerically<sup>11–13</sup>. So, due to the spin structure we have an analog of the well known Migdal theorem for electron-phonon interactions. This justifies SCBA according to which the hole Green's function satisfies a simple Dyson equation

$$G_d(\epsilon, \mathbf{k}) = \left( \epsilon - \epsilon_{0\mathbf{k}} - \sum_{\mathbf{q}} g_{\mathbf{k}-\mathbf{q},\mathbf{q}}^2 G_d(\epsilon - \omega_{\mathbf{q}}, \mathbf{k} - \mathbf{q}) + i0 \right)^{-1}. \quad (12)$$

The anomalous Green's function  $-i\langle 0 | T d_{\mathbf{k}\uparrow}(t) d_{\mathbf{k}\downarrow}^\dagger(0) | 0 \rangle$  vanishes because the  $z$ -projection of spin is conserved. Due to the definition of the operators (3) the Green's function (5) is invariant under translation with the inverse vector of the magnetic sublattice  $\mathbf{Q} = (\pm\pi, \pm\pi)$

$$G_d(\epsilon, \mathbf{k} + \mathbf{Q}) = G_d(\epsilon, \mathbf{k}). \quad (13)$$

The numerical solution of equation (12) is straightforward. As usual, to avoid poles we replace  $i0 \rightarrow i\Gamma/2 = i0.1$ . The energy scale consists of 300 points with variable density (concentrated near sharp structures of  $G_d$ ). The number of points in the magnetic Brillouin zone is  $10^4$  which is equivalent to the lattice  $140 \times 140$ . The plots of  $-\frac{1}{\pi} \text{Im } G_d(\epsilon, \mathbf{k})$  as a functions of  $\epsilon$  for  $\mathbf{k} = (\pi/2, \pi/2)$ ,  $\mathbf{k} = (\pi/2, 0)$ ,  $\mathbf{k} = (\pi, 0)$ , and  $\mathbf{k} = (0, 0)$  are presented in Fig.1. We recall that we use the set of parameters (2) based on Ref.<sup>5</sup>. The position of the lowest peak gives the quasiparticle energy. Results of the calculation can be fitted by the formula

$$\begin{aligned} \epsilon_{\mathbf{k}} &= \text{const} + \beta_1 \gamma_{\mathbf{k}}^2 + \beta_2 (\gamma_{\mathbf{k}}^-)^2 + \beta'_2 (\gamma_{\mathbf{k}}^-)^4 \\ \beta_1 &\approx 3.0, \quad \beta_2 \approx 3.8, \quad \beta'_2 \approx -1.5. \end{aligned} \quad (14)$$

The dispersion has minima at  $(\mathbf{k}_0 = (\pm\pi/2, \pm\pi/2))$ . The hole pockets are slightly stretched along the direction to the zone center, and it is very different from a pure  $t - J$  model<sup>11,12</sup>. The quasiparticle residue  $Z_{\mathbf{k}}^d$  can be found as the area under the peak. At the dispersion minimum it equals  $Z_{\mathbf{k}_0}^d = 0.38$ . So it is larger than in a pure  $t - J$  model<sup>11,12</sup>, but away from the dispersion minimum it drops down very rapidly. Plots of the residue  $Z_{\mathbf{k}}^d$  as a function of  $\mathbf{k}$  for  $\mathbf{k} \in [(\pi/2, \pi/2) - (0, 0)]$  and  $\mathbf{k} \in [(\pi/2, \pi/2) - (0, \pi)]$  are given at Fig. 2. Throughout the Brillouin zone the residue is fitted by

$$Z_{\mathbf{k}}^d = Z_{\mathbf{k}_0}^d \left( 1 - 0.9\gamma_{\mathbf{k}}^2 - 1.52(\gamma_{\mathbf{k}}^-)^2 + 0.05\gamma_{\mathbf{k}}^4 + 0.69(\gamma_{\mathbf{k}}^-)^4 + 0.5(\gamma_{\mathbf{k}}\gamma_{\mathbf{k}}^-)^2 \right). \quad (15)$$

### III. HOLE GREEN'S FUNCTION WITH FIXED SPIN. DYSON EQUATION RELATING TWO GREEN'S FUNCTIONS

The operators  $d_{\mathbf{k}\uparrow}$ ,  $d_{\mathbf{k}\downarrow}$  discussed in the previous section are defined at different sublattices. However, when a photon kicks out an electron from the system it does not separate the sublattices. Therefore for this process we have to define the operator as a simple Fourier transform

$$c_{\mathbf{k}\sigma} = \sqrt{\frac{2}{N}} \sum_i c_{i\sigma} e^{i\mathbf{k}\mathbf{r}_i}. \quad (16)$$

The normalization is chosen in such a way that  $\langle 0 | c_{\mathbf{k}\uparrow}^\dagger c_{\mathbf{k}\uparrow} | 0 \rangle = \frac{2}{N} \langle 0 | \sum_i c_{i\uparrow}^\dagger c_{i\uparrow} | 0 \rangle = 1$ . We can consider  $c_{\mathbf{k}\sigma}$  as an external perturbation, and the corresponding Green's function is

$$G_c(\epsilon, \mathbf{k}) = -i \int \langle 0 | T c_{\mathbf{k}\sigma}^\dagger(\tau) c_{\mathbf{k}\sigma}(0) | 0 \rangle e^{i\epsilon\tau} d\tau. \quad (17)$$

This is the Green's function measured in ARPES. Let us now find the relation between  $G_c(\epsilon, \mathbf{k})$  and  $G_d(\epsilon, \mathbf{k})$ .

The operator  $c_{\mathbf{k}\sigma}$  acting on the vacuum (ground state of the Heisenberg model) can produce a single hole state. We denote the corresponding amplitude by  $a_{\mathbf{k}}$  and show it in Fig. 3a as a cross. The thick line corresponds to the Green's function  $G_c$  (17) and the thin line corresponds to the  $G_d$  (5). The amplitude  $a_{\mathbf{k}}$  equals

$$a_{\mathbf{k}} = \langle 0 | d_{\mathbf{k}\uparrow} c_{\mathbf{k}\downarrow} | 0 \rangle = \langle 0 | \left( \sqrt{\frac{2}{N(1/2+m)}} \sum_{j\in\downarrow} c_{j\downarrow}^\dagger e^{-i\mathbf{k}\mathbf{r}_j} \right) \left( \sqrt{\frac{2}{N}} \sum_i c_{i\downarrow} e^{i\mathbf{k}\mathbf{r}_i} \right) | 0 \rangle = \sqrt{1/2+m}. \quad (18)$$

The operator  $c_{\mathbf{k}\sigma}$  acting on the vacuum can also produce a hole + spin-wave state. This amplitude is shown in Fig. 3b as a circled cross with the dashed line being a spin-wave. We denote this amplitude by  $b_{\mathbf{k},\mathbf{q}}$

$$\begin{aligned} b_{\mathbf{k},\mathbf{q}} &= \langle 0 | \beta_{\mathbf{q}} d_{\mathbf{k}-\mathbf{q}\downarrow} c_{\mathbf{k}\downarrow} | 0 \rangle = \langle 0 | \beta_{\mathbf{q}} \left( \sqrt{\frac{2}{N(1/2+m)}} \sum_{i\in\uparrow} c_{i\uparrow}^\dagger e^{-i(\mathbf{k}-\mathbf{q})\mathbf{r}_i} \right) \left( \sqrt{\frac{2}{N}} \sum_j c_{j\downarrow} e^{i\mathbf{k}\mathbf{r}_j} \right) | 0 \rangle \approx \\ &\approx \frac{2}{N} \langle 0 | \beta_{\mathbf{q}} \left( \sum_{i\in\uparrow} S_i^+ e^{i\mathbf{q}\mathbf{r}_i} \right) | 0 \rangle = \sqrt{\frac{2}{N}} v_{\mathbf{q}}. \end{aligned} \quad (19)$$

We stress that (19) is a bare vertex. It corresponds to the instantanious creation of a hole + spin wave, but not the creation of a hole with a subsequent decay into hole + spin-wave. To elucidate this point look at Fig.4. The upper part of this figure describes the wave function

of the initial Neel state: a - component without spin quantum fluctuations, b - component with spin quantum fluctuation. The lower part of Fig.4 arises immediately from the upper one after kicking out an electron with spin up. Part a does not contain a spin flip, and it corresponds to the amplitude  $a_{\mathbf{k}}$  (18). Part b does contain a spin flip, and it corresponds to the amplitude  $b_{\mathbf{k},\mathbf{q}}$  (19). Note that  $b_{\mathbf{k},\mathbf{q}} \rightarrow \infty$  at  $\mathbf{q} \rightarrow 0$ . The reason is that the operator (16) does not correspond to any quasiparticle of the system with long-range antiferromagnetic order, and therefore the usual Goldstone theorem is not applicable.

Let us denote by a dot (Fig. 3c) the usual hole-spin-wave vertex  $g_{\mathbf{k},\mathbf{q}}$  given by eq. (11). In the leading in  $t$  approximation the amplitude of single hole creation by the external perturbation (16) is given by diagrams presented at Fig. 5, with the thin solid line in this case the bare hole Green's function (7). If we set  $t' = t'' = 0$  and  $\epsilon = \epsilon_{0\mathbf{k}} = 0$  calculation of this amplitude can be easily done analytically

$$\begin{aligned} M_1(\epsilon = 0, \mathbf{k}) &= a_{\mathbf{k}} + \sum_{\mathbf{q}} \frac{b_{\mathbf{k},\mathbf{q}} g_{\mathbf{k}-\mathbf{q},\mathbf{q}}}{\epsilon_{0\mathbf{k}} - \epsilon_{0\mathbf{k}-\mathbf{q}} - \omega_{\mathbf{q}}} = \sqrt{0.8} - \frac{8t}{N} \sum_{\mathbf{q}} \frac{v_{\mathbf{q}}(\gamma_{\mathbf{k}-\mathbf{q}} u_{\mathbf{q}} + \gamma_{\mathbf{k}} v_{\mathbf{q}})}{\omega_{\mathbf{q}}} = \\ &= \sqrt{0.8} + \frac{4t}{N} \gamma_{\mathbf{k}} \sum_{\mathbf{q}} \left( \frac{1}{\omega_{\mathbf{q}}} - \frac{1}{2} \right) = \sqrt{0.8} (1 + 0.45 \cdot t \cdot \gamma_{\mathbf{k}}). \end{aligned} \quad (20)$$

$M_1^2$  is the quasiparticle residue of the Green's function (17). The eq. (20) agrees with the result obtained using a string representation<sup>15</sup>. We stress that even at  $t = 0$  the residue is 0.8 due to the spin quantum fluctuation in the ground state of the Heisenberg model<sup>16,17</sup>

Now we can find the relation between Green's functions  $G_c$  (17) and  $G_d$  (5). In the leading in  $t$  approximation it is given by diagrams presented at Fig. 6 with the thin solid line being in this case the bare hole Green's function  $G_{0d}$  (7). Now let us dress these diagrams by higher orders in hopping  $t$ . As we already discussed there is no single loop correction to the “dot”. We neglect double loop correction to the “dot” as it has been done in SCBA. Therefore the only possibility is an introduction of a self energy corrections. An example of the correction to diagram Fig. 6c is shown at Fig. 7. To take into account all these corrections we need just to replace at Fig. 6 all bare hole Green's functions (7) by dressed hole Green's function given by eq. (12). So, the Fig. 6 actually represents a Dyson equation relating  $G_c$  (17) and  $G_d$  (5). In analytical form it is

$$\begin{aligned} G_c(\epsilon, \mathbf{k}) &= a_{\mathbf{k}}^2 G_d(\epsilon, \mathbf{k}) + \sum_{\mathbf{q}} b_{\mathbf{k},\mathbf{q}}^2 G_d(\epsilon - \omega_{\mathbf{q}}, \mathbf{k} - \mathbf{q}) + \\ &+ 2a_{\mathbf{k}} G_d(\epsilon, \mathbf{k}) \left[ \sum_{\mathbf{q}} b_{\mathbf{k},\mathbf{q}} g_{\mathbf{k}-\mathbf{q},\mathbf{q}} G_d(\epsilon - \omega_{\mathbf{q}}, \mathbf{k} - \mathbf{q}) \right] + \\ &+ G_d(\epsilon, \mathbf{k}) \left[ \sum_{\mathbf{q}} b_{\mathbf{k},\mathbf{q}} g_{\mathbf{k}-\mathbf{q},\mathbf{q}} G_d(\epsilon - \omega_{\mathbf{q}}, \mathbf{k} - \mathbf{q}) \right]^2. \end{aligned} \quad (21)$$

So as soon as we have found  $G_d$  using SCBA (12) we can calculate the Green's function  $G_c$  defined by eq. (17). The imaginary part of  $G_c(\epsilon, \mathbf{k})$  gives directly the spectra measured in ARPES experiments.

We now discuss sum rules. All singularities of Green's functions are in the lower half plane of complex  $\epsilon$ . Therefore if we integrate eq.(12) over  $\epsilon$  from  $-\infty$  to  $+\infty$ , this integral can be replaced by the integral over an infinite semi-circle in the upper  $\epsilon$  half plane. For infinite  $\epsilon$ ,  $G_d = G_{0d}$ , and we get the well known sum rule

$$-\frac{1}{\pi} \text{Im} \int_{-\infty}^{\infty} G_d(\epsilon, \mathbf{k}) d\epsilon = 1, \quad (22)$$

which agrees with eq.(4). If we integrate now eq.(21) in the same limits, the terms which contain more than one Green's function give zero contribution, because the integral can be transferred into the upper complex  $\epsilon$  half plane. And we find

$$-\frac{1}{\pi} \text{Im} \int_{-\infty}^{\infty} G_c(\epsilon, \mathbf{k}) d\epsilon = \left( -\frac{1}{\pi} \text{Im} \int G_d(\epsilon, \mathbf{k}) d\epsilon \right) \left( a_{\mathbf{k}}^2 + \sum_{\mathbf{q}} b_{\mathbf{k}, \mathbf{q}}^2 \right) = 0.8 + \frac{2}{N} \sum_{\mathbf{q}} v_{\mathbf{q}}^2 = 1. \quad (23)$$

Thus the equation (21) reproduces the correct normalization:  $\langle 0 | c_{\mathbf{k}\uparrow}^\dagger c_{\mathbf{k}\uparrow} | 0 \rangle = 1$ .

The vertex  $b_{\mathbf{k}, \mathbf{q}}$  (19) is invariant under translation with the inverse vector of magnetic sublattice  $\mathbf{Q} = (\pm\pi, \pm\pi)$ :  $b_{\mathbf{k}+\mathbf{Q}, \mathbf{q}} = b_{\mathbf{k}, \mathbf{q}}$ . At the same time the vertex  $g_{\mathbf{k}, \mathbf{q}}$  (11) changes sign with this translation:  $g_{\mathbf{k}+\mathbf{Q}, \mathbf{q}} = -g_{\mathbf{k}, \mathbf{q}}$ . Therefore the diagrams Fig. 6c,d change sign at  $\mathbf{k} \rightarrow \mathbf{k} + \mathbf{Q}$  and

$$G_c(\epsilon, \mathbf{k} + \mathbf{Q}) \neq G_c(\epsilon, \mathbf{k}). \quad (24)$$

Due to the same properties of vertices  $b_{\mathbf{k}, \mathbf{q}}$  and  $g_{\mathbf{k}, \mathbf{q}}$  the diagrams Fig. 6c,d,e (square brackets in eq. (21)) vanish at the face of magnetic Brillouin zone ( $\gamma_{\mathbf{k}} = 0$ ). The diagram presented at Fig. 6b (term with  $b_{\mathbf{k}, \mathbf{q}}^2$  in eq. (21)) is small numerically. Therefore at the face of magnetic Brillouin zone  $G_c(\epsilon, \mathbf{k}) \approx G_d(\epsilon, \mathbf{k})$ . However away from the face they differ significantly. The plots of  $-\frac{1}{\pi} \text{Im} G_c(\epsilon, \mathbf{k})$  as a functions of  $\epsilon$  for  $\mathbf{k} = (\pi/2, \pi/2)$ ,  $\mathbf{k} = (\pi/2, 0)$ ,  $\mathbf{k} = (\pi, 0)$ , and  $\mathbf{k} = (0, 0)$  are presented at Fig.8. A plot of the quasiparticle residue  $Z_{\mathbf{k}}^c$  as a function of  $\mathbf{k}$  along (1,1) direction is given at Fig. 9. The quasiparticle residue outside the magnetic zone is smaller than that inside. For comparison we also present a plot of  $Z_{\mathbf{k}}^d$ .

#### IV. HUBBARD MODEL CORRECTION

The picture considered above corresponded to a modified  $t - J$  model. It means that double electron occupancy was forbidden. Now we want to take into account the fact that

the  $t - t' - t'' - J$  model originates from the Hubbard model. We assume that it is a simple one band Hubbard model with on site repulsion  $U$ . First of all this gives some corrections to the “bare” hole dispersion (6), see, e. g. Ref.<sup>4</sup>. However we assume that renormalization is done and these corrections are already included in the values of effective hopping amplitudes  $t', t''$  given in (2). There are also some corrections to the hole-spin-wave vertex<sup>4</sup>, but they are small at  $t', t'' \ll U$ . The really important effect is the renormalization of the vertex  $a_{\mathbf{k}}$  (18). In  $t - J$  model this vertex is given by the process shown at Fig. 10a: an electron is removed from corresponding sublattice. In Hubbard model there is an additional possibility shown at Fig. 10b: first the electron hops to occupied nearest site, and then it is removed from this site. Simple calculation shows that this gives

$$\begin{aligned} a_{\mathbf{k}} \rightarrow a_{\mathbf{k}} \times \left(1 + \frac{4t}{U}\gamma_{\mathbf{k}}\right) &= \sqrt{1/2 + m} \left(1 + \frac{J}{t}\gamma_{\mathbf{k}}\right), \\ b_{\mathbf{k},\mathbf{q}} \rightarrow b_{\mathbf{k},\mathbf{q}} \times \left(1 + \frac{4t}{U}\gamma_{\mathbf{k}}\right) &= \sqrt{\frac{2}{N}} v_{\mathbf{q}} \left(1 + \frac{J}{t}\gamma_{\mathbf{k}}\right). \end{aligned} \quad (25)$$

We took into account that  $J = 4t^2/U$ . The magnitude of the  $t/U$  correction in (25) is obvious, however one should be careful with the sign. To find it one needs to commute fermionic operators in order corresponding to Fig. 10b. The Dyson equation (21) remains valid. So we can easily find the Green’s function  $G_c^H$ , where index  $H$  indicates that the Hubbard model correction is taken into account. The plots of  $-\frac{1}{\pi} \text{Im } G_c^H(\epsilon, \mathbf{k})$  as functions of  $\epsilon$  for  $\mathbf{k} = (\pi/2, \pi/2)$ ,  $\mathbf{k} = (\pi/2, 0)$ ,  $\mathbf{k} = (\pi, 0)$ , and  $\mathbf{k} = (0, 0)$  are presented in Fig. 11. A plot of the quasiparticle residue  $Z_{\mathbf{k}}^{cH}$  as a function of  $\mathbf{k}$  along (1,1) direction is given in Fig. 9. We see that the “Hubbard correction” causes the decrease of the residue outside of the magnetic Brillouin zone to be steeper.

The sum rule (23) is changed. Now we have

$$-\frac{1}{\pi} \text{Im} \int_{-\infty}^{\infty} G_c^H(\epsilon, \mathbf{k}) d\epsilon \approx \left(1 + \frac{J}{t}\gamma_{\mathbf{k}}\right)^2 \approx 1 + 2\frac{J}{t}\gamma_{\mathbf{k}}. \quad (26)$$

Let us comment on the definition (16) of the operator  $c_{\mathbf{k}\sigma}$ . Its normalization is adjusted for a system with strong antiferromagnetic correlations and it is close to that for  $d_{\mathbf{k}\sigma}$  (see eq.(3)). However as a result the definition (16) differs from that usually accepted for a normal Fermi liquid by a factor  $\sqrt{2}$ . This is the reason why the sum rule (26) can be larger than unity. Generally the normalization can be chosen arbitrarily. It is a question of convenience only. However, let us prove that the sum rule for the total number of electrons in the system is fulfilled. According to definition (16)

$$c_{\mathbf{k}\sigma}^\dagger c_{\mathbf{k}\sigma} = 2N_{\mathbf{k}\sigma}, \quad (27)$$

where

$$N_{\mathbf{k}\sigma} = \left( \sqrt{\frac{1}{N}} \sum_i c_{i\sigma}^\dagger e^{-i\mathbf{k}\mathbf{r}_i} \right) \left( \sqrt{\frac{1}{N}} \sum_j c_{i\sigma} e^{i\mathbf{k}\mathbf{r}_j} \right) \quad (28)$$

is the operator for the number of electrons. Due to the definition (17) of Green's function  $G_c$  one has the standard relation

$$-\frac{1}{\pi} \text{Im} \int_{-\infty}^{\infty} G_{c,\sigma}^H(\epsilon, \mathbf{k}) d\epsilon = \langle 0 | c_{\mathbf{k}\sigma}^\dagger c_{\mathbf{k}\sigma} | 0 \rangle = 2 \langle 0 | N_{\mathbf{k}\sigma} | 0 \rangle. \quad (29)$$

Comparing with (26) we find

$$\langle 0 | N_{\mathbf{k}\sigma} | 0 \rangle = \frac{1}{2} \left( 1 + 2 \frac{J}{t} \gamma_{\mathbf{k}} \right). \quad (30)$$

The operator for the total number of electrons is equal to

$$\hat{N} = \sum_{\sigma, \mathbf{k} \in \text{full}} N_{\mathbf{k}\sigma}. \quad (31)$$

We put a “hat” to distinguish this operator from the number of sites  $N$ . Note that in all equations before we assumed summation over momenta inside the magnetic Brillouin zone. But in the eq. (31) we must sum over the full Brillouin zone. Finally from eqs. (30),(31) one finds that the sum rule for the total number of electrons

$$\langle 0 | \hat{N} | 0 \rangle = \sum_{\sigma, \mathbf{k} \in \text{full}} \frac{1}{2} \left( 1 + 2 \frac{J}{t} \gamma_{\mathbf{k}} \right) = N \quad (32)$$

is fulfilled. In conclusion of this discussion we would like to note that the origin of all these complications with normalization is very simple: The natural zone for the operator  $d_{\mathbf{k}\sigma}$  is the magnetic Brillouin zone. On the other hand the natural zone for  $c_{\mathbf{k}\sigma}$  is the full Brillouin zone. This is the reason why one should be careful comparing these two operators.

## V. COMPARISON WITH EXPERIMENT

Many of the experimental features observed are reproduced with the theory described here. The large dispersion between  $(0, 0)$  and  $(\pi/2, \pi/2)$  and the assymetric quasi particle weight about  $(\pi/2, \pi/2)$  with the very strong dcrease in weight on moving beyond  $(\pi/2, \pi/2)$ . Also the lack of dispersion along  $(0, 0)$  and  $(\pi, 0)$  as well as the very low quasiparticle weight is well reproduced. A major discrepancy between theory and experiment concerns the width of the quasi particle peak. The theoretical spectra (Figs. 8,11) have narrow peaks. On the

other hand the widths of the experimental ARPES spectra<sup>1</sup> are rather large,  $\Gamma_0 \approx 0.3eV \approx 2.4J$ . Although the experiment has been done at higher temperature  $T = 350K$  this is probably too low to explain the widths of the peaks in terms of excited spin waves. It seems that another degree of freedom not considered in the present work must be of importance. One such possibility is the coupling to phonons. Such a coupling is expected to be quite large for the cuprates especially for the Cu-O breathing mode since this strongly influences the stability of the Zang-Rice singlets. The coupling to phonons will result in a broadening of the quasi particle peak which can be described in terms of the Franck - Condon factors describing the probability that the system is left behind with a number of excited phonons upon the sudden removal of one electron<sup>18,19</sup>. Such a large width would indicate a strong coupling with phonons. In this paper we simulated the broadening with a Lorentz curve with a width  $\Gamma_0$ . The spectra obtained by convolution of  $-\frac{1}{\pi} \text{Im } G_c^H(\epsilon, \mathbf{k})$  with the broadening curve are given in Fig. 12. Agreement of these spectra with experimental ones<sup>1</sup> is quite reasonable.

## VI. CONCLUSIONS

In the present work we consider a modified  $t - J$  model at zero doping (insulating copper oxide plane) and zero temperature. We discuss the hole Green's functions with given pseudospin and given spin and derive a Dyson equation relating these two Green's functions. The Green's function with given pseudospin is very convenient for calculations, but it is an artificial object. In the real experiment one measures the hole Green's function with given spin.

To describe the experiment we use hopping amplitudes for a modified  $t - J$  model as obtained from LDA band calculations by Andersen *et al*<sup>5</sup>. Agreement of the theoretical spectra with experimental ones<sup>1</sup> is quite reasonable after some broadening of the theoretical spectra. The physical origin of this broadening is not quite clear. Possible explanations are in finite temperature, and the contributions due to phonons and the electron phonon interactions.

## VII. ACKNOWLEDGMENTS

We are very grateful to D. Khomskii, D. C. Mattis and D. Poilblanc for stimulating discussions, and A. Chernyshev for communicating the results prior to publication. One of

us (O. P. S.) acknowledge the Laboratoire de Physique Quantique, Universite Paul Sabatier; Materials Science Center, University of Groningen; and Institute for Theoretical Atomic and Molecular Physics at Harvard University (NSF grant PHY94-07194) for hospitality and support during work on the present problem.

## REFERENCES

<sup>a</sup> On leave from School of Physics, The University of New South Wales, Sydney 2052, Australia.

<sup>b</sup> Also at the Budker Institute of Nuclear Physics, 630090 Novosibirsk, Russia

<sup>1</sup> B. O. Wells *et al*, Phys. Rev. Lett. **74**, 964 (1995).

<sup>2</sup> J. J. Pothuizen *et al*, Phys. Rev. Lett. **78**, 717 (1997).

<sup>3</sup> A. Nazarenko, K. J. E. Vos, S. Haas, E. Dagotto, and R. J. Gooding, Phys. Rev. B **51**, 8676 (1995).

<sup>4</sup> J. Bala, A. M. Oles, and J. Zaanen, Phys. Rev. B **52** 4597 (1995).

<sup>5</sup> O. K. Andersen *et al*, J. Phys. Chem. Solids **56** 1573 (1995).

<sup>6</sup> A. L. Chernyshev, private communication.

<sup>7</sup> Y. Tokura *et al*, Phys. Rev. B **41**, 11657 (1990).

<sup>8</sup> M. Greven *et al*, Phys. Rev. Lett. **72** 1096 (1994).

<sup>9</sup> S. Schmitt-Rink, C. M. Varma, and A. E. Ruckenstein, Phys. Rev. Lett. **60**, 2793 (1988).

<sup>10</sup> C. L. Kane, P. A. Lee, and N. Read, Phys. Rev. B **39**, 6880 (1989).

<sup>11</sup> G. Martinez and P. Horsch, Phys. Rev. B **44**, 317 (1991).

<sup>12</sup> Z. Liu and E. Manousakis, Phys. Rev. B **45**, 2425 (1992).

<sup>13</sup> O. P. Sushkov, Phys. Rev. B **49**, 1250 (1994).

<sup>14</sup> E. Manousakis, Rev. Mod. Phys. **63**, 1 (1991).

<sup>15</sup> R. Eder and K. Becker, Phys. Rev. B **44**, 6982 (1991).

<sup>16</sup> A. G. Mal'shukov and G. D. Mahan, Phys. Rev. Lett. **68**, 2200 (1992).

<sup>17</sup> D. Poilblanc, T. Ziman, H. J. Schulz, E. Dagotto, Phys. Rev. B **47** 14267 (1993).

<sup>18</sup> G. Sawatzky, Nature **342**, 480 (1989).

<sup>19</sup> A. S. Alexandrov and N. F. Mott, High temperature superconductors and other superfluids, page 147. Taylor and Francis, 1994, London.

Figure captions,

Fig.1 Plots of  $-\frac{1}{\pi} \text{Im } G_d(\epsilon, \mathbf{k})$  for different values of  $\mathbf{k}$ . The Green's function is calculated in the self consistent Born approximation.

Fig.2 Quasiparticle residue  $Z_{\mathbf{k}}^d$  of the hole Green's function  $G_d$ . Solid line corresponds to the direction to the Brillouin zone center:  $\mathbf{k} \in [(\pi/2, \pi/2) - (0, 0)]$ . Dashed line gives dependence along the face of the magnetic Brillouin zone:  $\mathbf{k} \in [(\pi/2, \pi/2) - (0, \pi)]$ .

Fig.3 The vertices: a) - single hole creation, b) - hole + spin-wave creation, c) - usual hole-spin-wave vertex. Thick line correspond to  $G_c$ , and thin solid line corresponds to  $G_d$ . Dashed line is spin-wave.

Fig.4 Hole production mechanisms. Upper part of the figure describes wave function of initial Neel state: a - component without spin quantum fluctuations, b - component with spin quantum fluctuation. Lower part of the figure arises instantly from the upper one after removal of an electron with spin up. Part a does not contain spin flip, and it corresponds to the amplitude  $a_{\mathbf{k}}$ . Part b does contain spin flip, and it corresponds to the amplitude  $b_{\mathbf{k}, \mathbf{q}}$ .

Fig.5 Zero and first order in  $t$  diagrams for hole photoproduction.

Fig.6 Dyson equation relating Green's functions  $G_c$  (thick solid line) and  $G_d$  (thin solid line).

Fig.7 An example of higher order correction which is taken into account in the Dyson equation (21).

Fig.8 Plots of  $-\frac{1}{\pi} \text{Im } G_c(\epsilon, \mathbf{k})$  for different values of  $\mathbf{k}$ . The Green's function is found from Dyson equation (21) relating  $G_c$  with that in self consistent Born approximation.

Fig.9 Dependence of quasiparticle residues on  $\mathbf{k}$  along (1,1) direction.

Fig.10 Mechanisms of an electron removal without spin flip: a) -  $t - J$  model, b) - Hubbard model correction.

Fig.11 Plots of  $-\frac{1}{\pi} \text{Im } G_c^H(\epsilon, \mathbf{k})$  for different values of  $\mathbf{k}$ . The Green's function is found from Dyson equation (21) relating  $G_c^H$  with that in self consistent Born approximation.

Fig.12 Theoretical spectra for several values of  $\mathbf{k}$ . Spectra obtained by convolution of  $-\frac{1}{\pi} \text{Im } G_c^H(\epsilon, \mathbf{k})$  with spreading imitated by the Lorentz curve.

Fig. 1

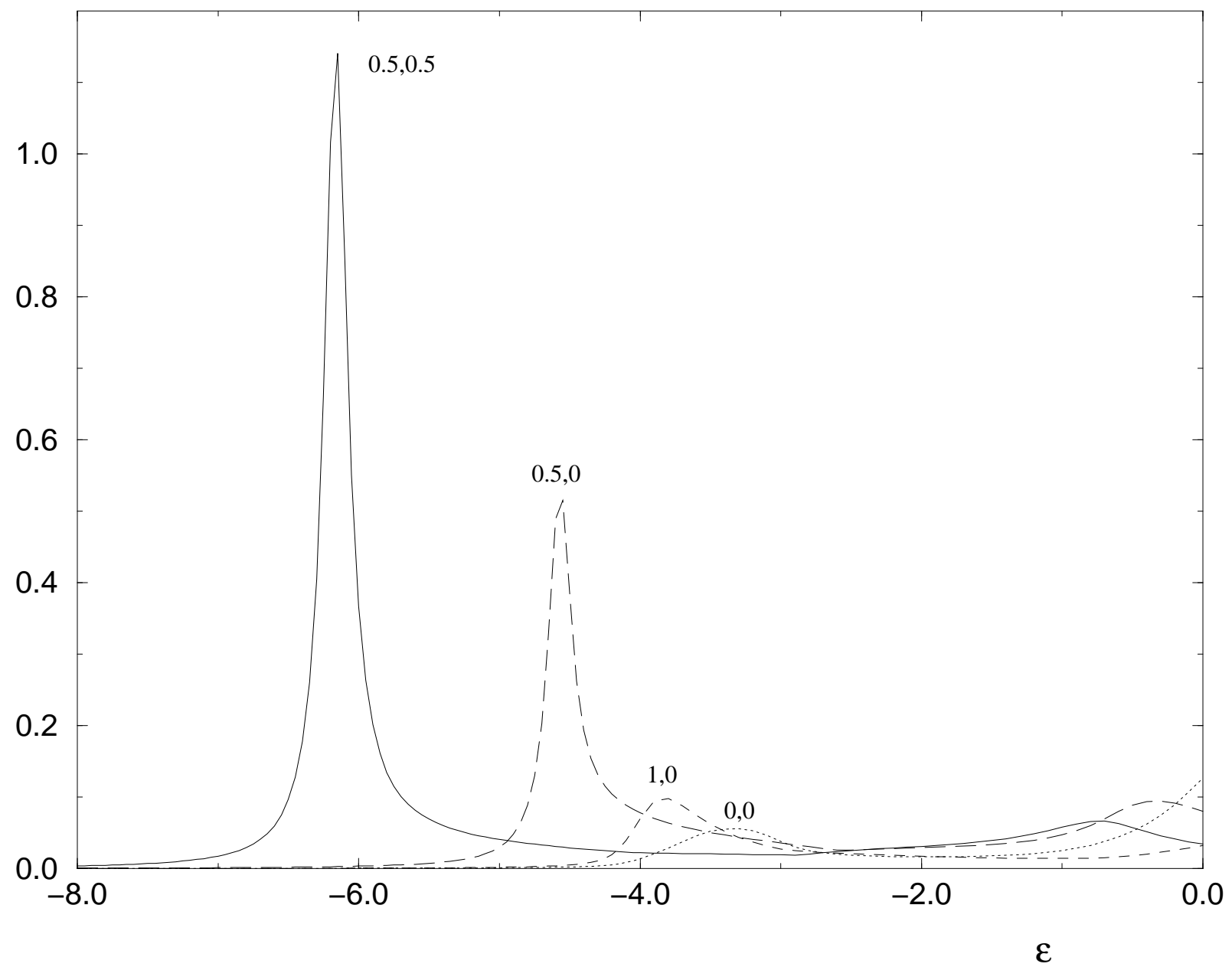


Fig. 1

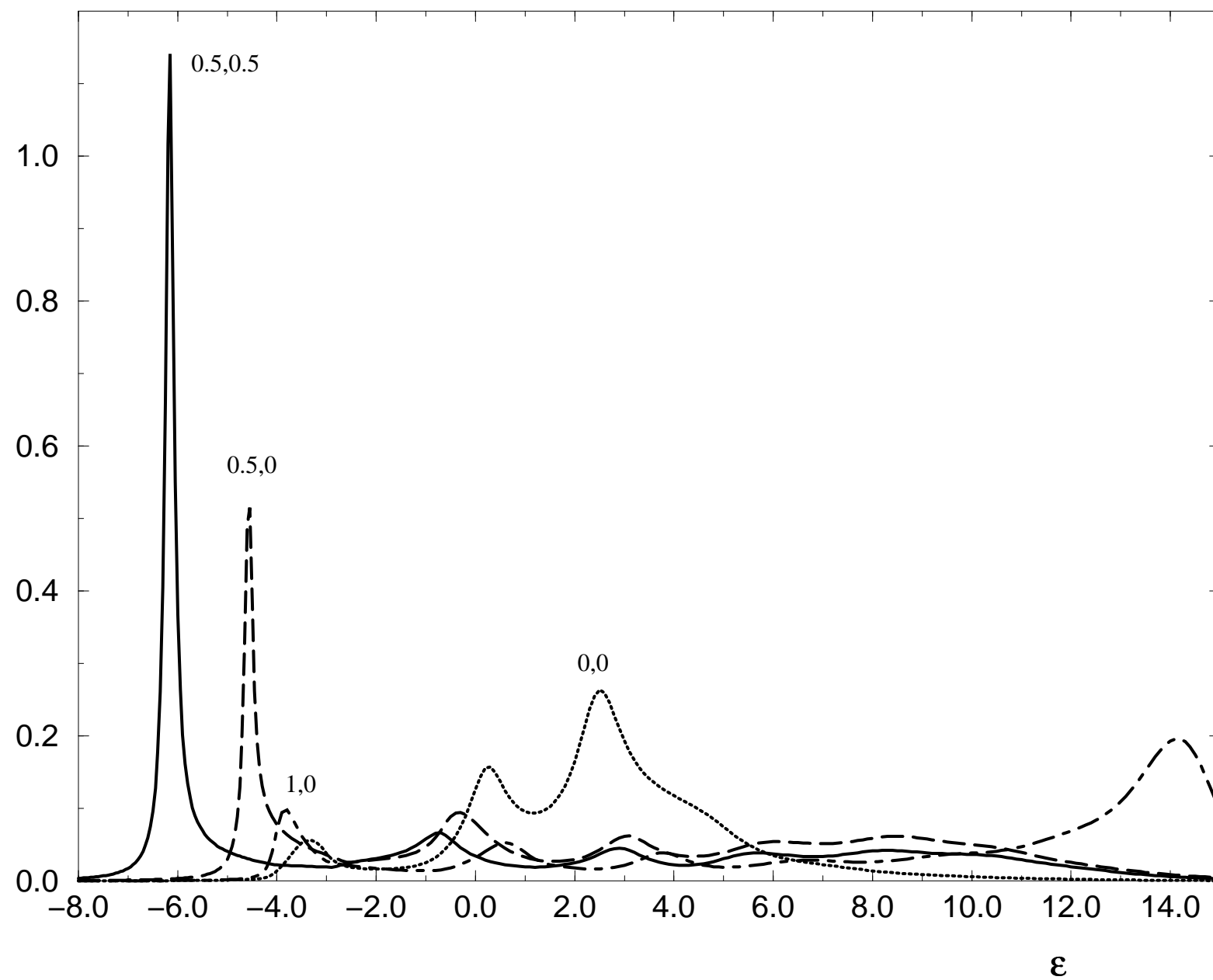
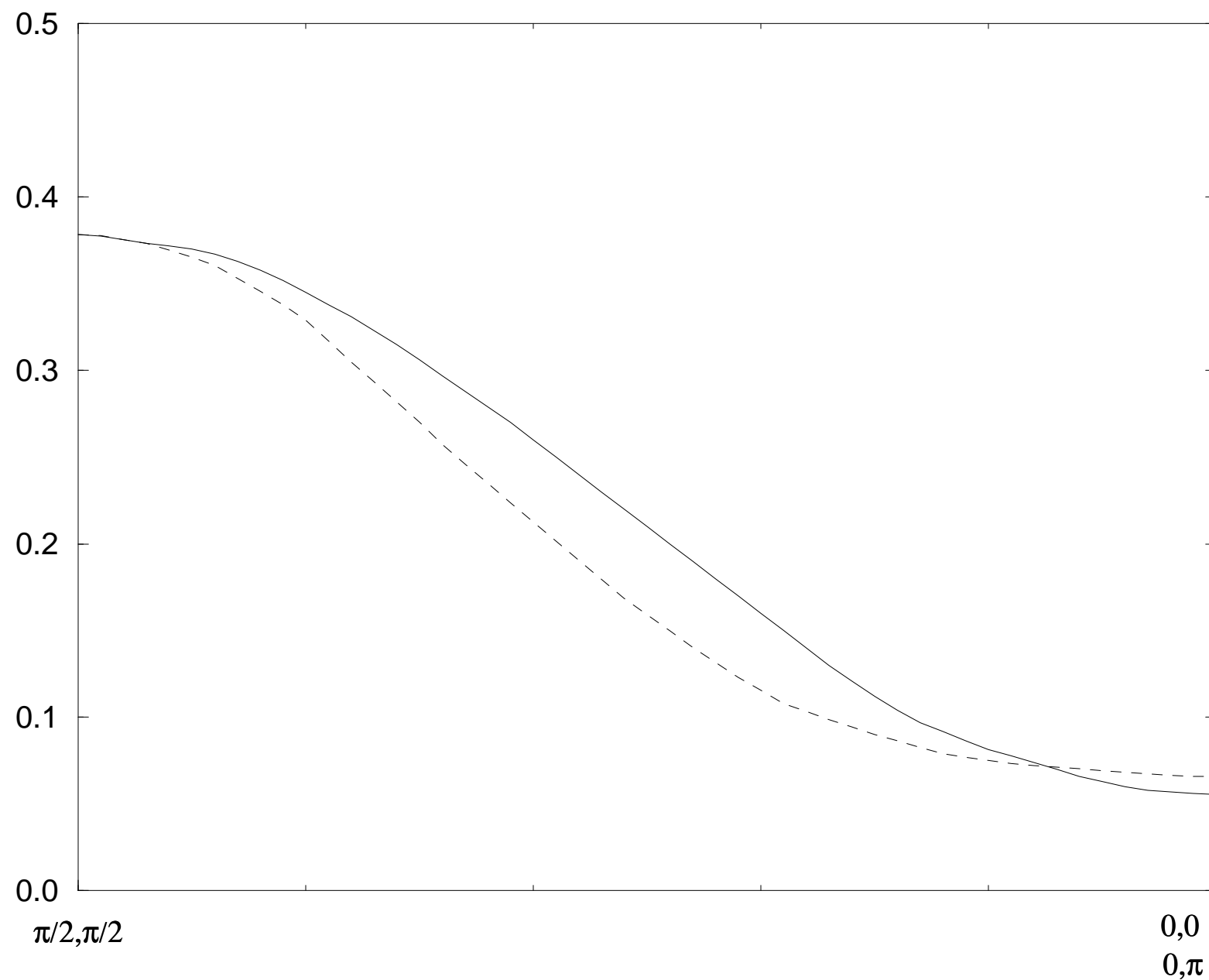
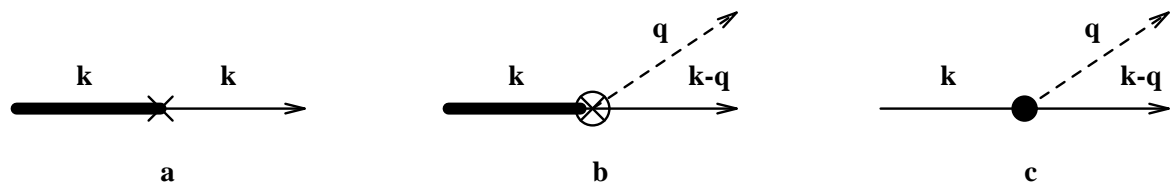
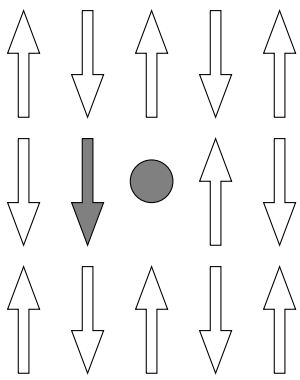
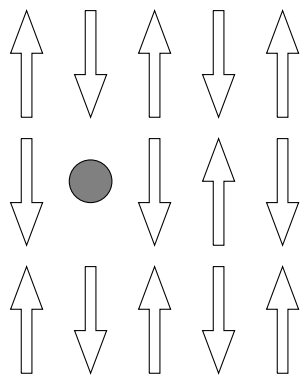
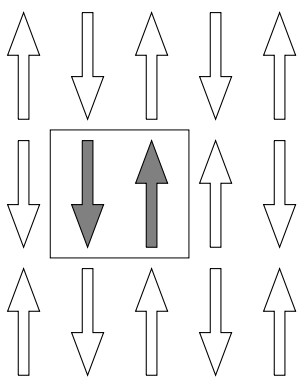
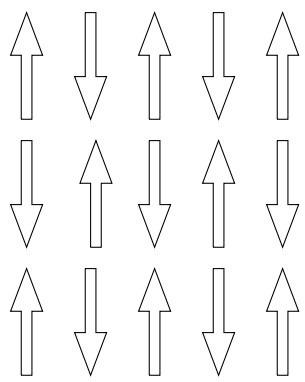


Fig. 2





**FIG. 3**



(a)

(b)



FIG. 5

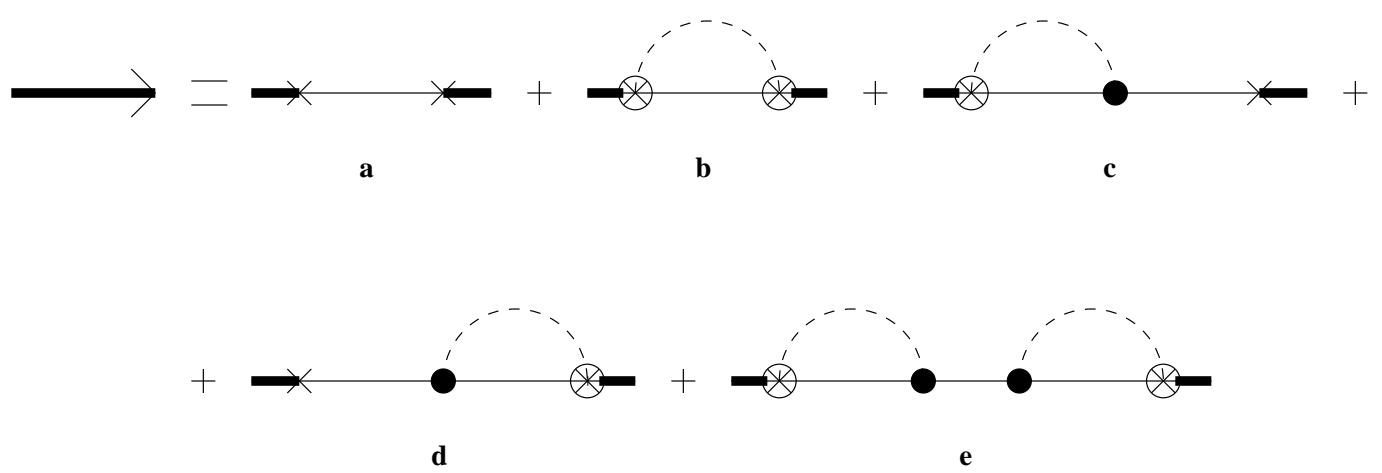


**FIG. 6**

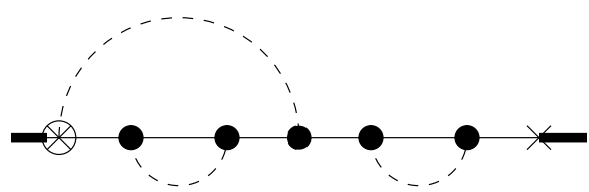


FIG. 7

Fig. 8

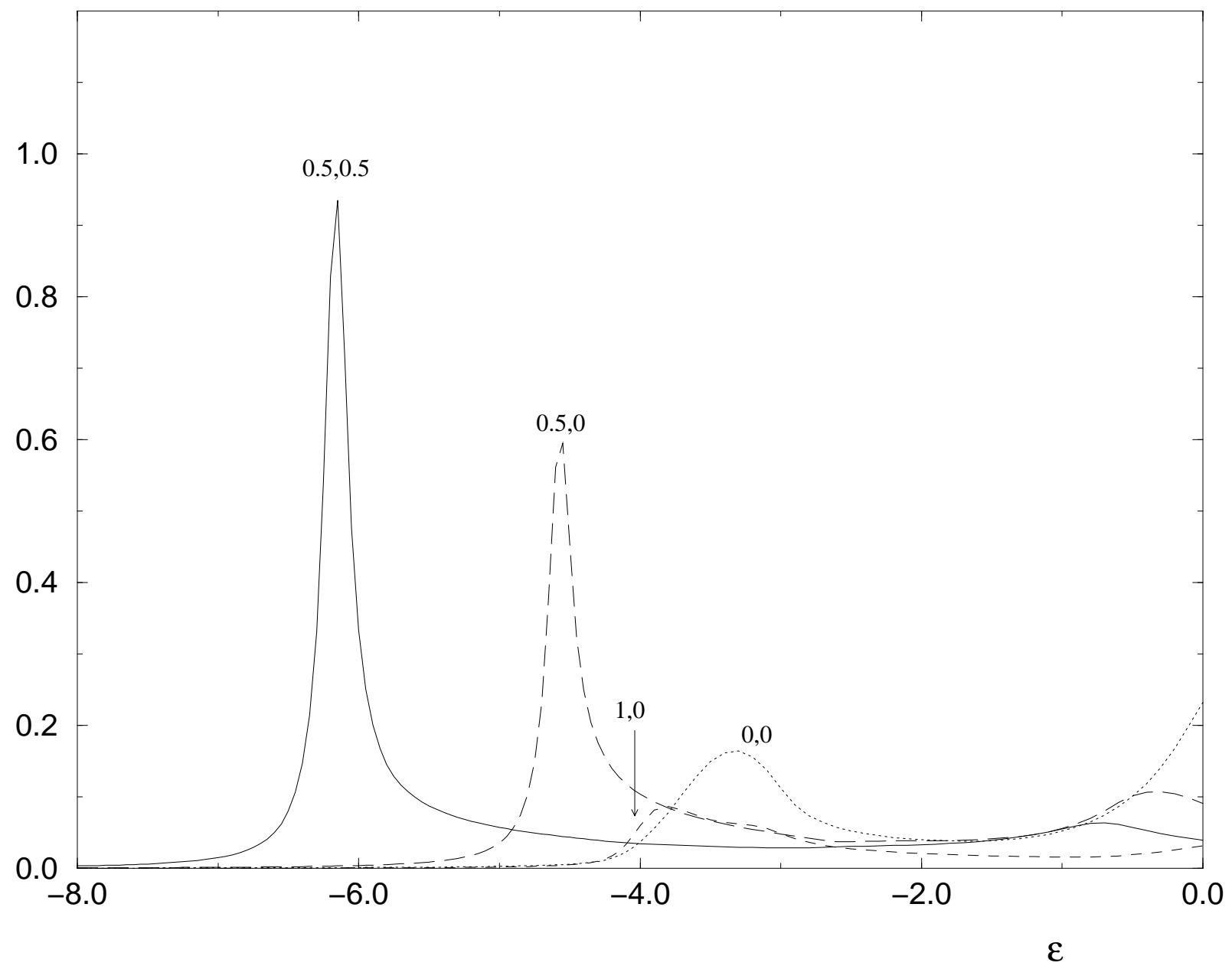
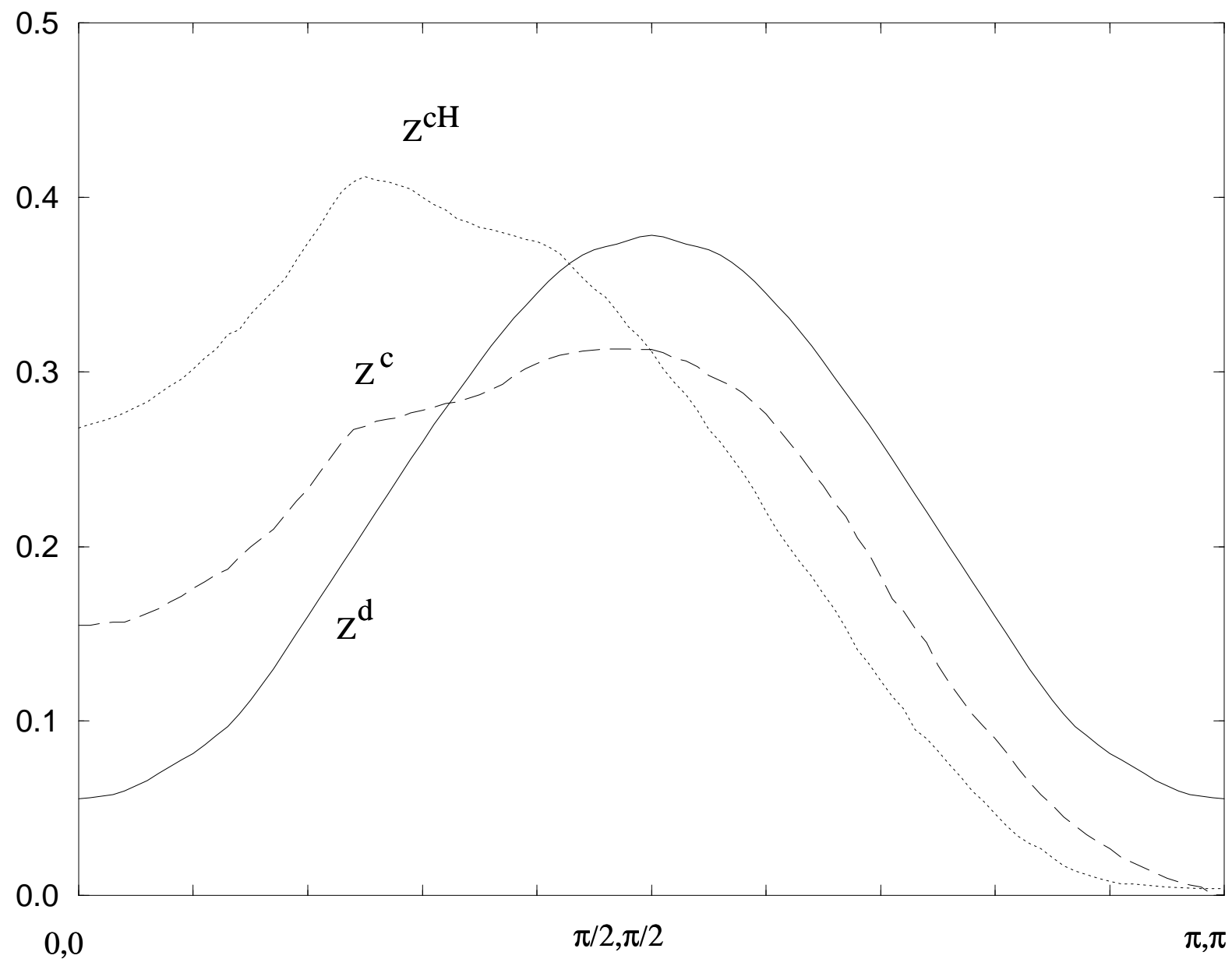


Fig. 9



$\uparrow \downarrow \uparrow \downarrow \longrightarrow \uparrow \downarrow \circ \downarrow$ **a** $\uparrow \downarrow \uparrow \downarrow \xrightarrow{\mathbf{t}} \uparrow \downarrow \circ \downarrow \longrightarrow \uparrow \downarrow \circ \downarrow$ **b****FIG. 10**

Fig. 11

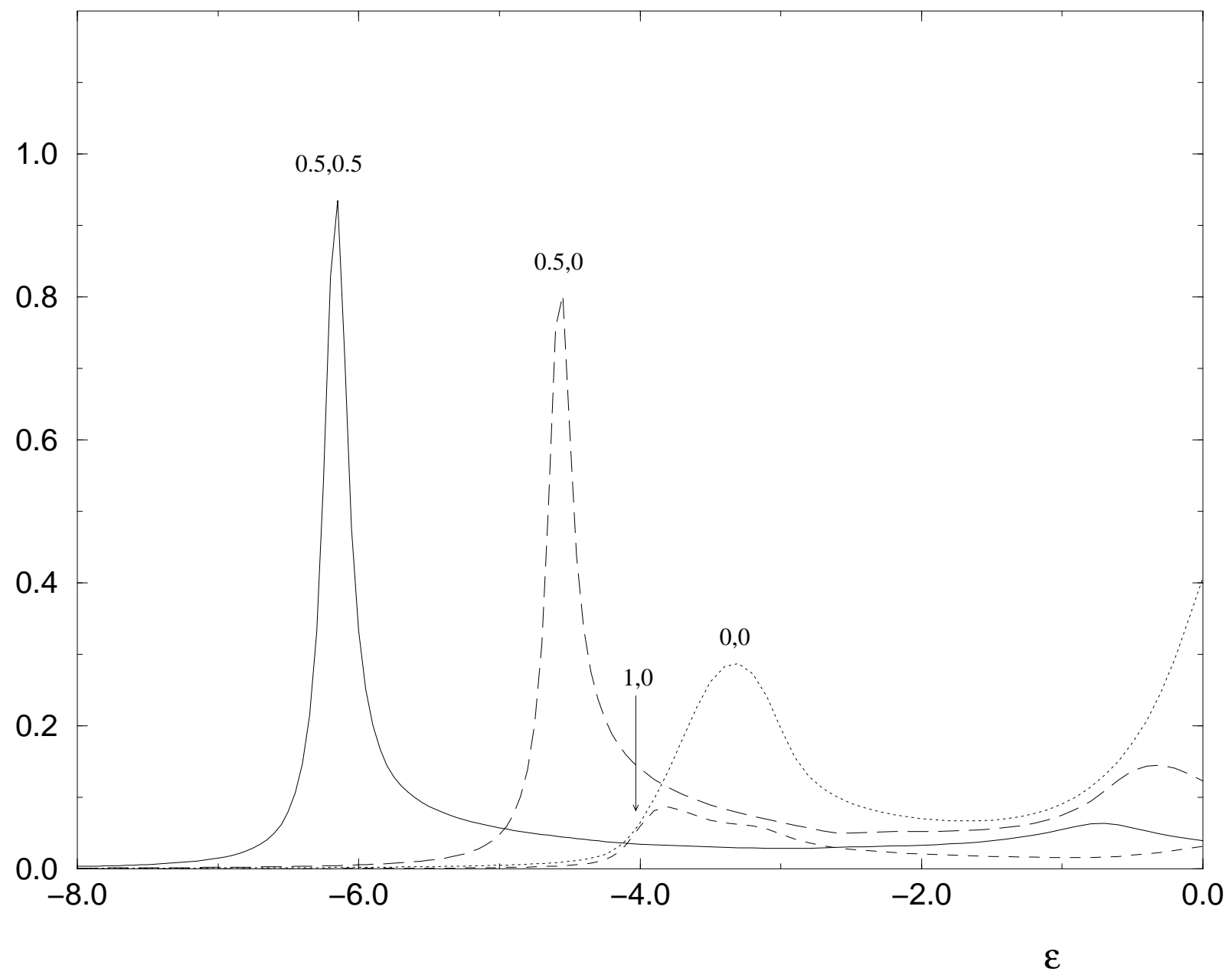


Fig. 12

